



Research article

UDC 621.3.019.32


DOI: 10.34910/MCE.137.9



## Evaluating the structural safety of steel frames using a probabilistic robustness index

A.V. Alekseytsev  , N.S. Kurchenko 

*Moscow State University of Civil Engineering (National Research University), Moscow, Russian Federation*

 [aalexw@mail.ru](mailto:aalexw@mail.ru)

**Keywords:** steel structures, robustness, mechanical safety, deformations, accident scenario, progressive collapse, reliability, failure probability, failure

**Abstract.** During the design of buildings and structures with steel frames, the issue of ensuring their mechanical safety under accidental actions arises. A number of such actions are not accounted for in the normal operating conditions of buildings and are therefore classified as emergency events. To assess the degree of resistance of load-bearing structures to these actions, the concept of structural robustness has been introduced in modern scientific literature. However, due to the insufficient study of the problem, there are relatively few works devoted to the quantitative assessment of robustness in the form of specific indicators, and those that do exist are primarily focused on reinforced concrete structures. This paper proposes a method for evaluating a probabilistic robustness index for steel frame structural systems. Its calculation uses a modified form of classical reliability theory equations, based on the premise that the failure of a frame system occurs through the formation of a mechanism with the minimum number of plastic hinges. When determining the probability of failure, the deformation behavior of frame elements is considered, with their sequential or parallel inclusion in the failure mechanism scheme, analogous to electrical circuits with series or parallel connections. To evaluate the dispersion of random variables, the statistical simulation method (Monte Carlo) and experimentally observed data are used. Examples of robustness index calculation are provided for various accident scenario types. The specific practical implementation of the method demonstrated its applicability, allowing conclusions to be drawn about the mechanical safety of structures with steel frame systems that are subject to heightened responsibility levels or other special requirements for resistance to progressive collapse.

**Citation:** Alekseytsev, A.V., Kurchenko, N.S. Evaluating the Structural Safety of Steel Frames Using a Probabilistic Robustness Index. Magazine of Civil Engineering. 2025. 18(5). Article no. 13709. DOI: 10.34910/MCE.137.9

### 1. Introduction

The problem of structural robustness in frame systems of buildings and structures constitutes a critical area of research in structural engineering, directly related to the assessment of mechanical safety. A review of recent studies has highlighted several key aspects of this issue:

- evaluation of structural robustness through the analysis of joint connections in structural elements;
- development and refinement of deterministic and probabilistic robustness indicators, as well as predictive systems based on artificial intelligence affecting progressive collapse scenarios;
- investigation of the mechanisms of progressive collapse using limit analysis and numerical methods;

- study of accidental actions, including single and multiple joint or element failures, fire exposure, corrosion damage, and seismic loading;
- robustness assessment and robustness-oriented design through search-based optimization algorithms, including multi-objective heuristic methods in combination with machine learning and artificial neural networks;
- development of structural solutions aimed at mitigating progressive collapse through force redistribution and energy dissipation;
- robustness and progressive collapse resistance in modular buildings with frame systems.

The following is a brief literature review on these thematic directions, which justifies the need for the development of a probabilistic robustness indicator, as proposed in the present study.

### *1.1. Robustness Assessment Based on joint Behavior Analysis*

The work in [1] focuses on the robustness of steel buildings with bolted connections as a function of their height. The analysis of 5-, 10-, and 15-story buildings revealed that taller buildings tend to exhibit greater structural robustness. The study emphasizes the importance of a probabilistic approach, which is implemented through the construction of fragility curves corresponding to progressive collapse scenarios. Studies [2, 3] emphasize that robustness is a key component of structural safety, particularly in steel moment-resisting frames where beam-to-column connections play a decisive role. Bolted corner connections are considered, and uncertainty in mechanical properties is addressed using the Monte Carlo simulation method. The study includes a vulnerability analysis of the structural system under accidental actions and develops tornado diagrams to determine sensitivity to various parameters such as span length, elastic modulus, and material strength, incorporating statistical modeling. In [4, 5], the performance of steel frame connections under bending moments is examined. The authors argue that ensuring ductile failure modes in joints can enhance both the robustness and reliability of structural systems. The inclusion of parameters that increase connection ductility is proposed as a mechanism to initiate progressive collapse arrest through plastic deformation localization. References [6, 7] investigate the behavior of steel frames subjected to sudden column removal, considering the influence of end plates in flange connections. The results demonstrate that end plates contribute to the localization of damage and enhance frame robustness under accidental scenarios. In [8–10], scenarios involving both instantaneous and gradual column loss in steel frames are explored. Structural robustness is linked to the integrity and robustness of joint connections. Both experimental and theoretical results confirm that flange dimensions play a crucial role in damage localization, thereby directly influencing robustness. The study in [11] examines the beam-to-column joint configuration and proposes enhancing robustness by enabling a reliable catenary action mechanism in frame systems. The authors suggest the use of slotted holes to improve joint ductility while maintaining strength. Experimental results confirm a significant increase in frame robustness.

### *1.2. Deterministic and Probabilistic Robustness Indicators; Artificial Intelligence Applications*

In [12, 13], a combined approach using structural analysis and artificial intelligence is applied to assess system robustness. Structural deformation data are interpreted using machine learning models under various accidental scenarios. The analysis indicates that selecting optimal structural geometry has a more pronounced effect on robustness than material strength enhancements. Studies [14, 15] introduce a safety index that accounts for uncertainties and supports design modifications to mitigate progressive collapse risks. It is shown that probabilistic modeling can reduce robustness estimates by up to 30 % compared to deterministic evaluations, with steel strength being a major contributing factor. Advanced damage detection tools such as artificial neural networks have also been employed [16], for example, to identify corrosion damage in steel components based on image analysis. In [17], a comprehensive robustness index is calculated for seismic-resilient buildings following AISC 360–16 guidelines. The index is defined as one minus the total material and non-material loss ratio, derived from dynamic analyses and fragility curve assessments [18]. Authors in [19] propose a robustness metric based on structural component strength, wherein strength degradation is linked to vulnerability. Both deterministic and probabilistic damage scenarios are considered, and it is concluded that systems with higher ductility exhibit superior robustness. Work [20] proposes a multi-criteria robustness index system incorporating energy-based, load-based, and stiffness-based metrics, with consideration for different progressive collapse patterns. Robustness is defined as the insensitivity of the system to local damage potentially initiating collapse.

In [21], robustness of steel structures is assessed using both deterministic approaches (applicable to seismic design according to [22]) and probabilistic models based on event trees. The resulting robustness index accounts for progressive collapse mechanisms and joint flexibility in moment frames.

### ***1.3. Mechanisms of Progressive Collapse***

Reference [23] evaluates the impact of initial local damage on the robustness of buildings made of cold-formed steel sections. It is shown that localized damage accelerates plastic hinge formation and reduces overall system resilience, especially in taller structures or those lacking corner and edge columns.

In [24], the classical definition of robustness is revised, and an alternative methodology based on plastic limit analysis (the method of ultimate equilibrium) is proposed. This eliminates the inaccuracies of quasi-static and full dynamic analyses in robustness assessment. Identification of damage or loading conditions serves as a foundation for determining real-life robustness indices [25]. For example, [26] presents a decision-tree algorithm based on vibration data and calibrated finite element models, capable of evaluating damage severity, robustness under extreme conditions, and residual life. Study [27] focuses on the fire resistance of steel structures under localized heating. While many studies address deformation and collapse mechanisms, reliable robustness assessment (both deterministic and probabilistic) must also account for structural strength as a mitigating factor against collapse propagation.

### ***1.4. Optimization of Parameters for Robustness Assessment***

Designs achieving specified robustness levels can be obtained through optimization techniques and analytical methods [28–30]. Standard heuristic algorithms [31–34] may be computationally expensive; therefore, hybrid methods combining stochastic search and neural networks are being developed. Metaheuristic optimization methods allow the exploration of various structural configurations to meet safety criteria [35]. These methods use multiple performance indicators, including economy, safety, and robustness [36]. In [37], group damage scenarios (e.g., simultaneous loss of several columns) are considered. Collapse propagation is predicted using a Pareto-based optimization model that minimizes initial energy input and maximizes resulting progressive damage. This dual-objective formulation enables quantification of system robustness and robustness. Similar to [35], combined algorithms (genetic algorithms, particle swarm optimization, neural networks) are used in [38] to optimize high-rise steel frame structures. Objectives may include internal force minimization and structural mass, facilitating robustness optimization under specific constraints. In [39], stress states and optimal joint design for tubular frame members are analyzed. Bio-inspired joint configurations (e.g., mimicking bamboo node geometry) are proposed to reduce stress concentration and enhance system durability and robustness.

### ***1.5. Investigation of Accidental Actions and Loading***

Metrics for evaluating the intensity of accidental actions, particularly seismic ones [40], include spectral accelerations and displacements, indirectly reflecting the system's robustness and highlighting its multi-parameter nature. The study compares robustness with respect to efficiency, practicality, and distance to the source of accidental action. Research in [41] explores fire-induced damage in steel frames, proposing localized fire analysis followed by frame-wide evaluation. Both interior and edge column failures are considered. In [42], a local-global analysis method is applied, where thermal effects act dynamically on a heated column, while the steel frame is treated under static assumptions. The method is shown to be applicable to frame systems made from various materials.

### ***1.6. Structural Solutions to Mitigate Progressive Collapse***

The study in [43] suggests enhancing robustness by installing a supplemental roof truss system capable of redistributing loads upon beam or column loss. The system is designed to yield and form plastic hinges under extreme loads. Numerical modeling provides recommendations for optimal stiffness values of truss elements. In [44], the presence or absence of bracing in steel frames is analyzed. Bracing increases ultimate load capacity by 129.7 % and 45.1 % in two frame variants, respectively, emphasizing its critical role in robustness. Robustness indicators here are evaluated in deterministic terms. Study [45] analyzes 50-story buildings designed to ASCE 7 and AISC standards. The impact of plan geometry on progressive collapse following column loss is investigated. Perimeter column removal leads to lower robustness indices compared to interior columns, while floor plan configuration has limited influence in the latter case. Further studies [46–47] assess robustness of tall buildings subjected to compound accidental scenarios, such as post-earthquake fire. Examples include 4- and 8-story frames with diagonal or V-shaped braces.

### ***1.7. Robustness and Progressive Collapse in Modular Buildings***

The study in [48] examines the progressive collapse resistance of modular buildings with columns, evaluating the role of beams, columns, and their joints. Beam characteristics (height, shear connectors, spacing) are shown to significantly affect robustness. Column reliability in frame systems is analyzed in [49]. Work [50] explores accidental loading on modular and frame structures under various joint configurations and both single and multiple damage scenarios. Enhanced joint strength improves robustness under isolated failures but remains a challenge for grouped failure scenarios. In [52], key factors influencing progressive collapse in modular buildings are identified, including load redistribution, failure

sequences, cross-section dimensions, bracing, and overturning effects. A design methodology incorporating robustness is proposed. Study [53] compares steel modular buildings under different module loss scenarios to traditional frames. It is shown that modular systems require significantly less material for floor systems while achieving comparable safety, indicating higher robustness. Similar evaluations for frame systems are conducted in [54]. The literature review confirms the relevance and insufficient exploration of probabilistic robustness assessment for steel moment-resisting frames, establishing the scientific basis and motivation for the current study.

## 2. Methods

### 2.1. Problem Statement

It is assumed that the robustness of a steel frame structure is ensured under the fulfillment of the following conditions:

- The condition of the static theorem of the plastic limit equilibrium method (A.A. Gvozdev) is satisfied, i.e., equilibrium is maintained in the damaged system with plastic hinges:

$$[K] \cdot \{\delta\} = \frac{1}{\alpha} \{P_0\} + \{P_M\}, \quad (1)$$

where:  $[K]$  is the global stiffness matrix of the finite element model;  $\{\delta\}$  is the vector of generalized nodal displacements;  $\{P_0\}$  is external load vector at  $\alpha = 1$ ,  $\{P_M\}$  is the equivalent load vector corresponding to the system of plastic moments in the plastic hinges;  $\alpha = P/P_{lim}$ ,  $P_{lim}$  is the critical load factor, at which the equilibrium condition is satisfied. The value of  $\alpha$  can be varied either directly or through modification of the external loading, requiring a corresponding update of the structural system. During this iterative process, additional plastic hinges may form, necessitating control based on the condition described below.

- The system retains geometric stability (geometric non-deformability) under both the initial impact and at the conclusion of the progressive collapse localization phase. This can be verified by evaluating the parameter  $\alpha_{cond}$ , computed from the condition number of the stiffness matrix of the damaged structure:

$$\alpha_{cond} = 1/cond_{\infty} [K], \quad (2)$$

where:  $cond_{\infty} [K] = \|[K]\|_{\infty} \times \|[K]^{-1}\|_{\infty}$  is the condition number of the stiffness matrix  $[K]$ ;  $\|\bullet\|_{\infty}$  is the infinity norm operator. Numerical studies indicate that high values of  $\alpha_{cond} < 10^{-16}$  are indicative of geometric instability. Specifically,  $10^{-10} < \alpha_{cond} < 10^{-2}$  implies instantaneously unstable behavior, while high but finite values suggest  $\alpha_{cond} > 10^3$  – conditioning and potential geometric deformability of the structure. It should be noted that a simpler yet sufficient criterion for assessing geometric invariability is the determinant condition: if  $\det[K] > 2$ , the system is geometrically stable. However, for large stiffness matrices – particularly in models containing solid (volume) finite elements – this approach can be computationally infeasible due to the high cost of matrix inversion required for determinant calculation. Loss of geometric stability may occur due to the initiation and propagation of cracks in welded joints or other critical elements of the structural nodes. The crack propagation process in structural steel may be approximately described using an energy-based formulation via the Cherepanov–Rice integral, resulting in a criterion for crack arrest upon damage initiation:

$$J = \int_C \left( W dy - \sigma_{iy} n_y \frac{\partial U_i}{\partial x} \right) dc \geq J_{cr}, \quad (3)$$

where:  $J$  is the contour integral [55];  $W$  is the strain energy density;  $\sigma_{iy}$ ,  $U_i$  are stresses and displacements components at point  $i$  in the  $y$  direction orthogonal to crack growth;  $n_y$  is unit normal vector;  $J_{cr}$  is the critical value of the  $J$ -integral corresponding to the fracture energy required to initiate or sustain crack propagation.

We adopt the assumption that the localization of the accidental action occurs primarily in the plane of maximum stiffness (i.e., the frame plane). Representative damage localization schemes with the formation of plastic hinges are shown in Fig. 1a–d.

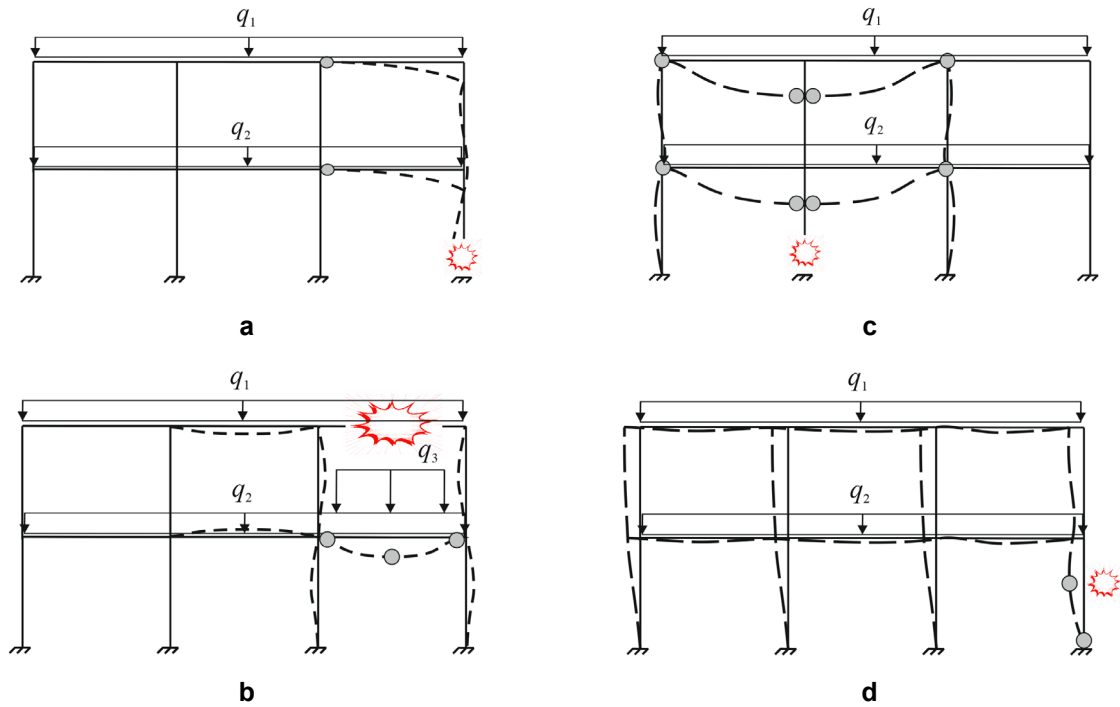


**Figure 1. Typical failure scenarios: a) failure of the edge column; b) failure of the middle column; c) failure of the beam followed by overloading of the lower floor; d) lateral impact on the end column without complete loss of load-bearing capacity. Plastic hinge locations are marked with gray circles.**

To formulate expressions for the reliability index and evaluate the performance of structural elements, we present the principal formulas for strength and global stability assessment (see Table 1). Local stability is not considered herein. For definiteness, we assume that all frame elements have solid I-shaped cross-sections; for columns, I- or W-sections are used. These profiles exhibit comparable out-of-plane and in-plane flexural stiffness, satisfying the requirements for both in-plane buckling resistance and out-of-plane global stability. In the following equations, the load factor  $\gamma_c = 1$  (coefficient of working conditions) is either assumed to be 1.0 or omitted entirely.

**Table 1. Strength design criteria for steel frame elements under accidental loading.**

Beams	Columns	Joints
<p>1. Strength of the element as part of the frame under combined compression and bending, <math>\sigma &lt; 440</math> MPa: calculated according to formula (106) of SP 16.13330.2017,</p> $\frac{(N / A_n \pm M_x y / I_{xn})}{R_y \gamma_c} \leq 1,$ <p>where all notations are provided.</p> <p>2. Global stability of the element as part of the frame under dynamic loading: according to formula (69) of SP 16.13330.2017</p> $\frac{M_x}{\varphi_b W_{cx} R_y \gamma_c} \leq 1$ <p>3. Shear strength at support sections: calculated by formula (42) of SP 16.13330.2017 for first-class stress-strain state (SSS) structures and by formulas (54)–(55) for second and third classes.</p>	<p>1. Global stability of the element as part of the frame under dynamic loading:</p> $\frac{N}{\varphi_e A R_y \gamma_c} \leq 1$ <p>calculated according to formula (109) of SP 16.13330.2017, considering the effective slenderness and reduced relative eccentricity, which are evaluated accounting for the material's dynamic characteristics and internal force values.</p> <p>2. Strength check according to formula (109) for short columns.</p>	<p>1. Welded connections: Strength verification of butt, fillet, and lap joints according to formulas (175)–(181) of SP 16.13330.2017.</p> <p>2. Bolted connections: For nodes subjected to maximum dynamic loading, apply formulas (186)–(188), (190) from SP 16.13330.2017.</p>

## 2.2. Reliability Indices for Probabilistic Robustness Assessment

Reliability indices for the strength of beams can be formulated using the criteria of normal and shear stresses, which determine the corresponding probabilities of failure due to bending, accounting for the axial force as part of the frame, and shear at support zones:

$$\beta_{\sigma} = \frac{|R_y| - |\sigma_{MN}|}{\sqrt{S(\tilde{\sigma}_{MN})^2 + S(\tilde{R}_y)^2}}, \quad \tilde{\sigma}_{MN} = \tilde{N}/A \pm \tilde{M}_x y/I_x, \quad \tilde{N} = f_1(\tilde{Q}), \quad \tilde{M}_x = f_2(\tilde{Q}); \quad (4)$$

$$\beta_{\tau} = \frac{|R_s| - |\tau_x|}{\sqrt{S(\tilde{\tau}_x)^2 + S(\tilde{R}_s)^2}}, \quad \tilde{\tau}_x = \begin{cases} \tilde{Q}_x S/I_x t_w - 1\text{-st class of SSS} \\ \tilde{Q}_x/A_w - 2\text{-nd, 3-rd classes of SSS} \end{cases}, \quad \tilde{Q}_x = f(\tilde{Q}), \quad (5)$$

where:  $\beta_{\sigma}$ ,  $\beta_{\tau}$  are reliability indices based on normal and shear stresses;  $\sigma_{MN}$ ,  $\tau_x$  are the expected values (means) of normal and shear stresses in critical sections;  $R_y$ ,  $R_s$  are the design resistances in bending and shear for structural steel;  $S(\bullet)$  is the standard deviation operator for random variables; internal forces  $\tilde{N}$ ,  $\tilde{M}_x$ ,  $\tilde{Q}_x$ ,  $\tilde{\sigma}_{MN}$ ,  $\tilde{\tau}_x$  (axial force, bending moment, shear force) and stresses (normal and shear) are considered as random variables obtained via statistical modeling;  $A$ ,  $S$ ,  $I_x$ ,  $t_w$ ,  $A_w$ ,  $y$  are the cross-sectional area, first moment of area, moment of inertia in the frame plane, web thickness, web area, and the coordinate of the stress evaluation point relative to the neutral axis;  $\tilde{Q}$  is the observed value of the random load, including accidental actions.

The functions  $f$ ,  $f_1$ ,  $f_2$  define the relationship between external load and internal forces and can be derived through machine learning models or iterative simulations with varying load levels.

In equation (4), the random variable of normal stress  $\sigma_{MN}$ , is composed of two components. Its standard deviation can be calculated as:

$$S(\sigma_{MN}) = \sqrt{D(\tilde{N}/A) + D(\tilde{M}_x y/I_x) + 2 \text{cov}((\tilde{N}/A), (\tilde{M}_x y/I_x))}; \quad (6)$$

$$\text{cov}((\tilde{N}/A), (\tilde{M}_x y/I_x)) = \frac{1}{n} \sum_{i=1}^n ((\tilde{N}\tilde{M}_x y)/(I_x A))_i - (\bar{\tilde{N}}/A)(\bar{\tilde{M}_x y/I_x}), \quad (7)$$

where:  $D(\bullet)$  is the variance operator;  $\text{cov}((\bullet), (\bullet))$  is the covariance operator;  $(\bar{\bullet})$  are sample means;  $n$  is the sample size defined in the simulation or based on tested specimens.

The reliability index for the global stability of a beam element is given by:

$$\beta_s = \frac{|R_y| - |\sigma_{Mx}|}{\sqrt{S(\tilde{\sigma}_M)^2 + S(\tilde{R}_y)^2}}, \quad \tilde{\sigma}_{Mx} = \frac{\tilde{M}_x}{\phi_b W_{cx}}, \quad (8)$$

where:  $\sigma_M$  is the expected value of conditional normal stress, considering axial force under bending;  $W_{cx}$  is the section modulus for the most compressed fiber in the frame plane;  $\phi_b$  is the stability coefficient as defined in SP 16.13330.2017, depending on the geometry of the I-section.

For columns subjected to dynamic axial and bending loads due to accidental actions, the stability reliability index is defined as:

$$\beta_{st} = \frac{|R_y| - |\sigma_N|}{\sqrt{S(\tilde{\sigma}_N)^2 + S(\tilde{R}_y)^2}}, \quad \tilde{\sigma}_N = \frac{\tilde{N}}{\phi_e A}, \quad (9)$$

where:  $\sigma_N$  is the expected value of conditional normal stress;  $\varphi_e$  is the combined stability coefficient depending on the slenderness ratio  $\bar{\lambda}$  and reduced eccentricity, adjusted by the section shape coefficient  $\eta$ .

If  $\varphi_e$  is treated as a random variable (due to its dependence on  $\tilde{N}$ ,  $\tilde{M}_x$ ), the standard deviation must be computed as:

$$S(\tilde{\sigma}_N) = \sqrt{D\left(\frac{\tilde{N}}{\varphi_e A}\right)} = \sqrt{D\left(\frac{\tilde{N}}{F\left(\eta\left(\tilde{M}_A/\tilde{N}W_c\right), \bar{\lambda}\right) A}\right)}. \quad (10)$$

However, since  $F\left(\eta\left(\tilde{M}_A/\tilde{N}W_c\right), \bar{\lambda}\right)$  is defined deterministically in Table D3 of SP 16.13330.2017, and its derivation lies outside the scope of this study, we treat  $\varphi_e$  as a deterministic quantity. The standard deviation  $S(\tilde{\sigma}_N)$  is thus calculated by:

$$S(\tilde{\sigma}_N) = \sqrt{\frac{1}{n(n-1)} \sum_{i=1}^n \left( \left( \frac{\tilde{N}}{\varphi_e A} \right)_i - \left( \frac{\tilde{N}}{\varphi_e A} \right) \right)^2}. \quad (11)$$

For short columns, where loss of stability may not occur, the reliability index can be computed using equation (4). For joint components, reliability indices can be formulated similarly. For example, in the case of welded butt joints, equation (9) can be used, replacing  $\sigma_N$  with  $\sigma_N = N/(t l_w)$ , where  $t$  is the weld leg length and  $l_w$  is the weld length. The design strength of the steel member  $R_y$  is replaced with the design strength of the weld metal  $R_{wy}$ .

### 2.3. Statistical Modeling of Random Variables

The standard deviations of the random variables representing loads and design resistances can be determined based on the collection of actual statistical data for structures of a certain type, as well as from test reports used to establish their actual mechanical characteristics. However, such data are not always available, and in a number of cases, statistical simulation methods are employed. In particular, for the problems considered herein, the standard deviations of the random variables of loads – and, consequently, the stresses induced by them – as well as the resistance of structural steel grade S375, are determined using statistical sampling methods. It is assumed that the scatter in the values of stresses and resistance is of the same order of magnitude. Therefore, to determine the standard deviations, it is sufficient to generate a basic sample  $\omega$  of values ranging from zero to one (see Table 3), based on experimental values of the coefficient of variation of the tensile strength of the steel under uniaxial loading. The histogram for these data is shown in Fig. 2. Subsequently, using the generated sample  $\omega$ , statistical realizations of the stress  $\sigma_{MN}$  and resistance  $R_y$  values are obtained based on the expressions  $\sigma_{MN,i} = \omega_i \bar{\sigma}_{MN}$ ,  $R_{y,i} = \omega_i \bar{R}_y$ , where  $\bar{\sigma}_{MN}$  and  $\bar{R}_y$  are the mathematical expectations, assumed, in particular, to be equal to the values of the maximum normal stress induced by external loading and the nominal resistance, respectively. Thus, by using the data of synthetic statistics with a normal distribution (or by processing data from full-scale experiments), it is possible to calculate reliability indices using formulas (4) and (5).

**Table 2. Sample set of  $\omega$  for determining root mean square standards for ultimate forces.**

$\omega_{1-10}$	$\omega_{11-20}$	$\omega_{21-30}$	$\omega_{31-40}$	$\omega_{41-50}$	$\omega_{51-60}$	$\omega_{61-70}$	$\omega_{71-80}$	$\omega_{81-90}$	$\omega_{91-100}$
0.690	0.691	0.008	0.490	0.398	0.775	0.314	0.069	0.841	0.838
0.672	0.485	0.459	0.604	0.410	0.297	0.699	0.736	0.215	0.875
0.132	0.026	0.514	0.924	0.474	0.612	0.801	0.845	0.918	0.831
0.750	0.429	0.064	0.695	0.358	0.344	0.162	0.523	0.926	0.557
0.992	0.534	0.675	0.708	0.775	0.725	0.671	0.042	0.762	0.465
0.414	0.997	0.562	0.186	0.367	0.877	0.650	0.655	0.865	0.405
0.569	0.286	0.527	0.834	0.162	0.213	0.212	0.752	0.725	0.390
0.758	0.470	0.540	0.716	0.090	0.435	0.717	0.913	0.973	0.306
0.893	0.234	0.194	0.149	0.520	0.755	0.356	0.015	0.061	0.006
0.783	0.304	0.593	0.101	0.579	0.947	0.591	0.575	0.065	0.098

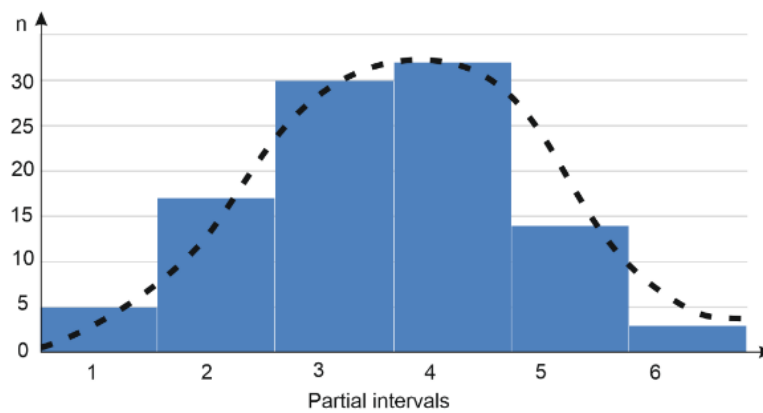


**Figure 2. Histogram of the sample data set;**  
 **$n$  – number of members (statistical variants) in interval length (1/6).**

#### 2.4. Probabilistic Robustness Index

For individual steel structural elements, the probabilistic robustness index can be defined, in a simplified case, as the product of the probabilities of failure-free performance under normal service conditions and under accidental loading:

$$w = P_{no} (1 - P_{dam}), \quad (12)$$

where:  $P_{no}$  is the probability of failure-free performance under service loads;  $P_{dam}$  is the probability of failure under accidental action. In structural design following standard procedures, the service reliability probability typically falls within the range  $P_{no} = 0.95 \div 1$ . In optimization procedures that do not explicitly account for accidental scenarios,  $P_{no} = 0.98 \div 1$ . For an “ideal” robustness condition, the robustness index is  $w_R = 1$ , meaning  $P_{no} = 1$ ,  $P_{dam} = 0$ . For a structural system in the form of a steel frame, the main topological components that may fail under accidental actions are:  $m_C$  columns,  $m_R$  beams, and  $m_U$  joints.

Let  $m_R$ ,  $m_C$  and  $m_U$  represent the number of beams, columns, and joints, respectively. Then, the system-wide probabilistic robustness index can be estimated as:

$$W_R = \prod_{i=1}^{m_R} (P_{no,i} (1 - P_{dam,i})) \prod_{j=1}^{m_C} (P_{no,j} (1 - P_{dam,j})) \prod_{k=1}^{m_U} (P_{no,k} (1 - P_{dam,k})), \quad (13)$$



where:  $P_{no,i}$ ,  $P_{no,j}$ ,  $P_{no,k}$  are the probabilities of failure-free performance for the  $i$ -th beam,  $j$ -th column, and  $k$ -th joint under service loads;  $P_{dam,i}$ ,  $P_{dam,j}$ ,  $P_{dam,k}$  are the probabilities of failure under accidental loads for the corresponding elements. These failure probabilities can be evaluated using the standard formula:

$$P_{dam} = 1 - (0.5 + \Phi(\beta)), \quad (14)$$

where:  $\Phi(\beta)$  is the cumulative distribution function of the standard normal distribution (Laplace function);  $\beta$  is the reliability index of the element or connection, which can be calculated based on equations (4)–(9).

If the maximum failure probability among all components satisfies the condition  $P_{dam}^{\max} = 0.5$ :  $\Phi(\beta) = 0$ ,  $\beta = 0$ , then the system is considered not robust. More generally, the system robustness is deemed compromised if failure-free performance is not ensured for at least one critical group of components:

$$\left( \prod_{i=1}^{m_R} (w_i) \right) \vee \left( \prod_{j=1}^{m_c} (w_j) \right) \vee \left( \prod_{k=1}^{m_U} (w_k) \right) = [0 \div 0.6]. \quad (15)$$

In a special case where all beams and joints remain operational but some columns fail, the system may still be considered survivable provided that  $W_R \geq 0.95 \cdot 0.6 \cdot 0.95 \approx 0.55$ . Different failure propagation scenarios due to accidental loading can be modeled analogously to electrical systems, using series or parallel system logic. For example, the failure probability of a sequence of three beams failing progressively (1–2–3) can be computed as:  $P_{dam} = P_{dam1} + P_{dam1} \cdot P_{dam2} + P_{dam1} \cdot P_{dam2} \cdot P_{dam3}$ . Each term in the sum corresponds to the failure probability of an individual beam assuming progressive collapse initiated by the preceding failure. If the condition (1) is violated or geometric instability is detected based on the condition number estimation in equation (2), then the probabilistic robustness index  $W_R$  becomes irrelevant, as the structure is collapsed.

### 3. Results

#### 3.1. General Information

The study considers a steel frame structure fabricated from steel with a yield strength of  $R_{yn} = 375$  MPa, the configuration of which is shown in Fig. 3.

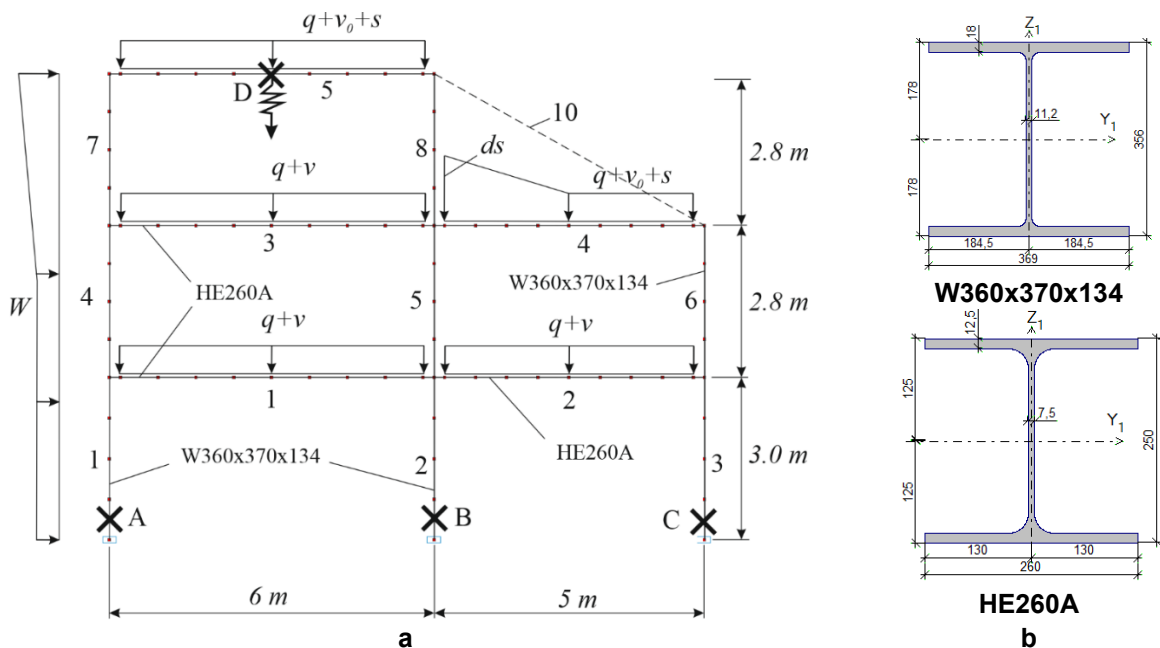


Figure 3. Calculation scheme of the frame (a): 1–12 – column numbers, 1–9 – beam numbers (from left to right by floors); design parameters of column sections and beams sections (b).

All columns in the frame are made of W360x370x134 profiles, and all beams are of type HE260A. Elements in the diagram are labeled by number, except for element 10. Potential accident scenarios are marked with crosses and involve progressive failure mechanisms through the formation of plastic hinges. Element 10 represents a diagonal member (shown with a dashed line) that is introduced to redistribute internal forces and enhance the robustness of the frame. This member is not present in the structure under normal service conditions.

It is believed that the destruction of a frame structure made of ductile steel with the formation of a mechanism with ductile joints is based on a consequence of the static theorem of the limit equilibrium method. That is, the system transitions to a state of geometric variability (mechanism) at such a minimum load that eliminates the degree of static indeterminacy by excluding angular connections, while in a statically determinate system with conditional plastic hinges, a limit state is observed in one of the sections. In this case, the number of plastic hinges is minimal.

The frame was designed for the following service loads: dead load:  $q = 40$  kN/m (including the frame elements and reinforced concrete slab); wind loads (considering both mean and pulsating components, from both directions – note that leeward wind load is not shown in the diagram for simplicity); snow load:  $s = 13.2$  kN/m for a Moscow region, including snow accumulation:  $ds = 39.6$  kN/m; live load on the floor slab:  $v = 9$  kN/m; live load on the roof:  $v_0 = 3$  kN/m. The design solutions shown in Fig. 2 include safety reserves in the profile section dimensions, which are assumed to be utilized under accidental scenarios. Table 2 presents a possible material consumption optimization without considering accidental events.

**Table 2. Design options for the frame focusing on safety.**

Structural members, Fig. 2	Original profile (safety)	Costs optimization results	Reduction of material consumption	Reduction of bending rigidity
Columns				
1, 4, 7	W360x370x134	HE260A	39%	68%
2, 5, 8	W360x370x134	HE300AA	37%	58%
3, 6	W360x370x134	HE260AA	38%	56%
Beams				
1	HE260A	HE240AA	30%	44%
2	HE260A	HE220AA	40%	60%
3	HE260A	HE240AA	30%	44%
4	HE260A	HE220AA	40%	60%
5	HE260A	HE240AA	30%	44%

### 3.2. Normal Operating Conditions

Since the frame members are long, the contribution of normal stresses predominates in their strength assessment. However, considering that in the critical sections of the beams both shear forces and moments reach their maximum values, it is advisable to use von Mises equivalent stresses, which account for the combined effect of normal and shear stresses (Fig. 4). These stresses are used to calculate reliability indices in Table 3.

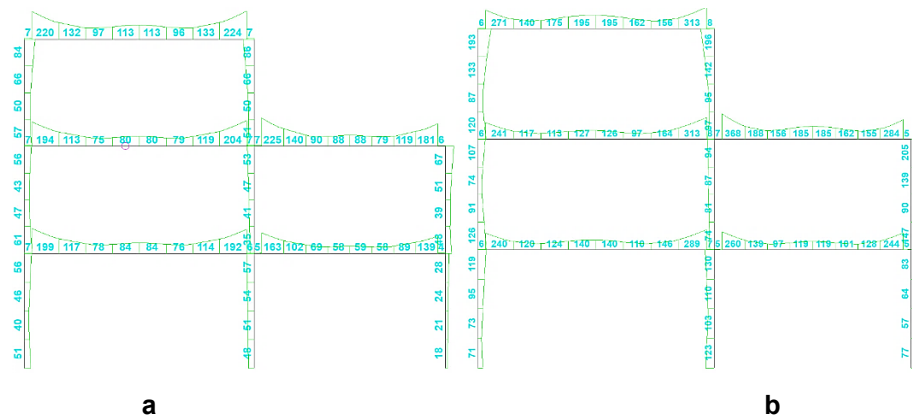


**Figure 4. Diagram of equivalent stresses (MPa) under normal operating conditions of the frame: a) design with allowance for possible accident; b) minimization of material consumption.**

**Table 3. To the calculation of the value  $P_{dam}$  (Scenario A).**

No. of the element	Original design, $\frac{\sigma_e / \varphi}{R_y}, \text{ MPa}$	Optimal design, $\frac{\sigma_{e,opt} / \varphi_{opt}}{R_y}, \text{ MPa}$	$\frac{\beta_R}{\beta_{Ropt}}$	$\frac{\Phi(\beta_R)}{\Phi(\beta_{Ropt})}$	$\frac{P_{dam,i}}{P_{dam,i,opt}}$
Columns					
1	56/337.5 <sup>1</sup>	119/300 <sup>2</sup>	$\frac{\beta_R > 5}{4.9}$	$\frac{0,5}{0.499997}$	$\frac{0}{3 \cdot 10^{-6}}$
2	57/337.5 <sup>1</sup>	130/320	$\frac{\beta_R > 5}{\beta_{Ropt} > 5}$	$\frac{0.5}{0.5}$	$\frac{0}{0}$
3	28/337.5 <sup>1</sup>	83/280	same	same	same
4	61/345 <sup>2</sup>	128/321	-//-	-//-	same
5	53/345	94/342	-//-	-//-	same
6	67/345	205/299	$\frac{\beta_R > 5}{2.47}$	$\frac{0,5}{0.4933}$	$\frac{0}{6.7 \cdot 10^{-3}}$
7	84/345	193/321	$\frac{\beta_R > 5}{3.36}$	$\frac{0.5}{0.49955}$	$\frac{0}{4.5 \cdot 10^{-4}}$
8	86/345	196/342	$\frac{\beta_R > 5}{3.84}$	$\frac{0,5}{0.499922}$	$\frac{0}{8.8 \cdot 10^{-5}}$
Beams					
1	192/375	289/375	$\frac{4.81}{2.26}$	$\frac{0.499997}{0.4881}$	$\frac{3 \cdot 10^{-6}}{1.19 \cdot 10^{-2}}$
2	163/375	260/375	$\frac{\beta_R > 5}{3.02}$	$\frac{0,5}{0.49863}$	$\frac{0}{1.37 \cdot 10^{-3}}$
3	204/375	313/375	$\frac{4.5}{1.63}$	$\frac{0.499997}{0.4484}$	$\frac{3 \cdot 10^{-6}}{5.16 \cdot 10^{-2}}$
4	225/375	368/375	$\frac{3.9}{0.18}$	$\frac{0.499948}{0.0714}$	$\frac{5.2 \cdot 10^{-5}}{0.4286}$
5	224/375	313/375	$\frac{4.0}{1.63}$	$\frac{0.499968}{0.4484}$	$\frac{3.2 \cdot 10^{-5}}{5.16 \cdot 10^{-2}}$

<sup>1</sup>Obtained:  $375 \cdot 0.9 = 337,5 - \varphi = 0.9$  longitudinal bending coefficient for beams.

<sup>2</sup>Obtained considering longitudinal bending coefficients depending on the column slenderness.

<sup>3</sup>Obtained by formula (4):  $(337.5 - 56) / 38 = 7.4$ , where  $\sqrt{S(\bar{\sigma}_M)^2 + S(\bar{R}_y)^2} \approx 38$  MPa was calculated using statistical modeling;  $\beta_{Ropt} = (300 - 113.5) / 38 = 4.9$ .

Analysis of Table 3 shows that optimization by the criterion of minimizing material consumption allows obtaining an economical solution, but the reliability of such a solution significantly decreases (by several orders of magnitude). There is a real probability of failure even due to factors related to the statistical nature of the mechanical properties of steel and load effects. We calculate the probabilities of failure-free operation of columns and beams (Table 4).

**Table 4. Calculation of the probability of failure-free operation of the system.**

Original design		Optimal design		Probability of frame failure-free operation	Risk of damage
Columns $P_{no,c} = \prod_{i=1}^8 P_{no,i}$	Beams $P_{no,b} = \prod_{i=1}^5 P_{no,i}$	Columns $P_{no,c} = \prod_{i=1}^8 P_{no,i}$	Beams $P_{no,b} = \prod_{i=1}^5 P_{no,i}$		
1	$0.999997 \cdot 1 \cdot 0.999997 \times$ $\times 0.999948 \cdot 0.999968 =$ $= 0.99991$	$0.999997 \cdot 1 \cdot 1 \cdot 1 \cdot 0.9933 \times$ $\times 0.99955 \cdot 0.999912 =$ $= 0.99276$	$0.9881 \cdot 0.99863 \cdot 0.9484 \times$ $\times 0.5714 \cdot 0.9484 =$ $= 0.50714$	$\frac{0.99991}{0.5034}$	$\frac{90}{496600}$

Table 4 illustrates that a design optimized solely by the criterion of minimum material consumption is significantly riskier, with the risk of material losses being several orders of magnitude higher compared to the original design. It should be noted that the failure of the frame in this case will likely not result in total collapse; rather, the failure is expected to occur at the support joint of the roof beam in the area of increased snow accumulation. Moreover, according to the results presented in Tables 3 and 4, it becomes evident that designs optimized for minimum steel consumption are not survivable under any accidental loads.

### 3.3. Accidental Scenarios: General Information

To demonstrate the effectiveness of robustness assessment based on a probabilistic indicator, two calculations are performed for each accidental scenario: one without element 10 (see Fig. 2), and one with this structural element included. The dynamic effects associated with support removal are modeled using a quasi-static approach, applying the G.A. Geniev effect, which involves multiplying the static internal forces in the damaged area by a dynamic load amplification factor. Only the original (non-optimized) design is considered. It is assumed that all joint connections in the frame structure remain fully functional under all configurations. The procedure for calculating the probabilistic robustness index of the frame involves the following steps:

- Estimation of the system's reliability under normal operation, which is computed as the product of the reliability values of individual elements. In traditional design practice, this value is close to unity, as shown in Section 3.2.
- Estimation of the reliability of beams and columns in the event of a column removal (in this case, a parallel failure model is applied to the frame elements).
- Estimation of the reliability of beams in the event of the removal of one of the beams while all columns remain intact (a series failure model is applied to the beams in this case).

#### 3.3.1. Accidental Scenario A

A linear static analysis is performed for the system with support A removed. In sections where stresses exceed the yield strength, plastic hinges are introduced. Next, the geometric stability of the system is evaluated in accordance with equation (2). The deformed configuration along with the pattern of plastic hinge formation for this accidental scenario is shown in Fig. 5a. An analysis of the stiffness matrix condition number indicates an immediate loss of stiffness, implying that the system lacks robustness.

However, the validity of this conclusion can be verified via nonlinear analysis, which accounts for both physical and geometric nonlinearities. This analysis was carried out using the SCAD software package (Fig. 5b). The stress-strain behavior was modeled using a Padé approximation of a bilinear deformation diagram, with a limiting strain value of 0.03. The results of this analysis show that, upon the removal of the support, the system transitions into a mechanism (i.e., collapses) when the applied load reaches approximately 80 % of the design service load. The resulting vertical deflection of the structure reaches 1.447 m.

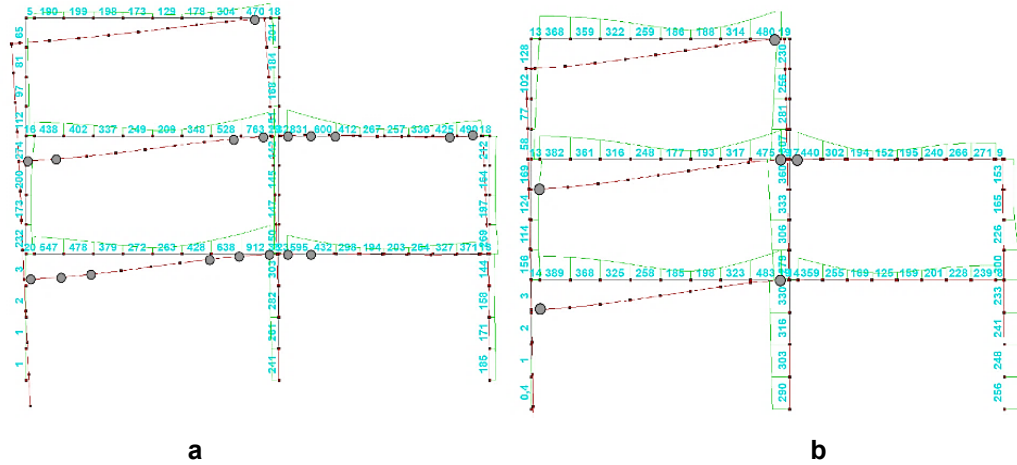


**Figure 5. Diagram of equivalent quasi-static stresses (MPa) for emergency conditions (a), results of physically and geometrically nonlinear calculation (b).**

**Table 5. Calculation of the values  $P_{dam}$  (Scenario A).**

No. of elements	$\frac{\sigma_e / \varphi}{R_y}$ , MPa	$\beta_R$	$\Phi(\beta_b)$	$P_{dam,i}$
Columns				
1	—	—	—	—
2	274/337.5	1.67	0.4525	0.0475
3	112/337.5	$\beta > 5$	0.5	0
4	303/345	1.1	0.3643	0.1357
5	150/345	$\beta > 5$	0.5	0
6	201/345	3.78	0.49991	$9.0 \cdot 10^{-5}$
7	185/345	4.21	0.49997	$3.0 \cdot 10^{-5}$
8	212/345	3.5	0.49977	$2.3 \cdot 10^{-4}$
Beams				
1	>1	0	0	0.5
2	371/375	0.1	0.0398	0.4602
3	>1	0	0	0.5
4	>1	0	0	0.5
5	304/375	1.86	0.4686	0.0315

Formula (10) takes the form:  $W_R = \prod_{i=1}^{m_R} (P_{no,i} (1 - P_{dam,i})) \prod_{j=1}^{m_c} (P_{no,j} (1 - P_{dam,j}))$ , using the data from Tables 4 and 5, obtained:

$$W_R \approx \left( 1 \left( 0.9525 \cdot 0.8643 \cdot 0.999991 \cdot 0.999997 \cdot 0.9977 \cdot 1^2 \right) \right) (0.999997 \cdot 0.5) (0.999997 \cdot 0.5398) \times \\ \times (0.999997 \cdot 0.5) (0.999997 \cdot 0.5) (0.999997 \cdot 0.9685) = 0.05375.$$

The robustness condition is not satisfied,  $W_R \approx 0.05375 \ll 0.55$ . This result indicates the inefficiency of structural measures aimed at increasing robustness. Therefore, instead of attempting to enhance the robustness of the damaged structure, efforts should be directed toward preventing the initiation of such an accidental scenario. In reality, even with the inclusion of element 10 in the analytical model (see Fig. 2), the

structure still failed at a load level of 0.8 of the critical accidental loads. However, the system deflection decreased to 1.156 m, and the robustness indicator  $W_R$  remained of the same order of magnitude.

### 3.3.2. Accidental Scenario B

Using the relationships from Table 1, or more generally, the von Mises energy-based strength criterion, the data necessary to determine the reliability index is computed (see Fig. 6).

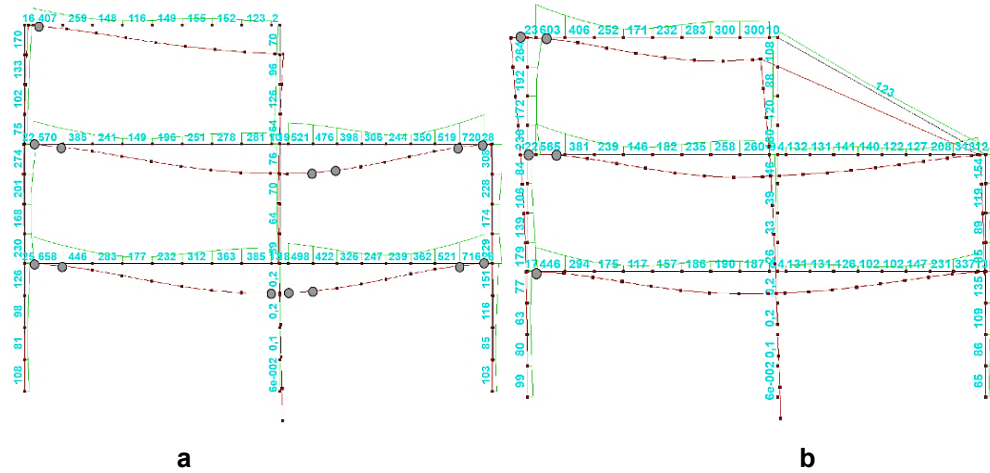


**Figure 6. Distributions of equivalent quasi-static stresses (MPa) and deformed configurations of the frame with formation of plastic hinges: a) without diagonal bracing; b) with diagonal bracing.**

An analysis of the condition number of the system's stiffness matrix in Fig. 6a revealed that the frame is instantaneously unstable, whereas the system in Fig. 6b is geometrically stable. However, instantaneous instability cannot be interpreted as a lack of robustness in general, since the localization of damage may lead to the formation of alternative load paths or chain mechanisms. Therefore, we proceed to evaluate the robustness of these systems using a probabilistic indicator, followed by verification of the results through physically and geometrically nonlinear analysis. The corresponding data are presented in Tables 6 and 7.

**Table 6. Calculation of the values  $P_{dam}$  (Scenario B).**

No. of elements	Frame on Fig. 6a,	Frame on Fig. 6b,	$\frac{\beta_1}{\beta_2}$ (fig. 6, a)	$\frac{\Phi(\beta_1)}{\Phi(\beta_2)}$	$\frac{P_{1dam,i}}{P_{2dam,i}}$
	$\frac{\sigma_e / \varphi}{R_y}$ , MPa	$\frac{\sigma_e / \varphi}{R_y}$ , MPa	$\frac{\beta_1}{\beta_2}$ (fig. 6, b)		
Columns					
1	126/337.5	99/337.5	$\frac{\beta_1 > 5}{\beta_2 > 5}$	$\frac{0.5}{0.5}$	$\frac{0}{0}$
2	—	—	—	—	—
3	151/337.5	135/337.5	$\frac{4.9}{\beta_2 > 5}$	$\frac{0.499997}{0.5}$	$\frac{3 \cdot 10^{-6}}{0}$
4	274/345	179/345	$\frac{1.86}{4.3}$	$\frac{0.4686}{0.499997}$	$\frac{0.0314}{3 \cdot 10^{-6}}$
5	76/345	48/345	$\frac{\beta_1 > 5}{\beta_2 > 5}$	$\frac{0.5}{0.5}$	$\frac{0}{0}$
6	308/345	154/345	$\frac{0.97}{\beta_2 > 5}$	$\frac{0.334}{0.5}$	$\frac{0.166}{0}$
7	170/345	264/345	$\frac{4.6}{2.13}$	$\frac{0.499997}{0.4834}$	$\frac{3 \cdot 10^{-6}}{0.0166}$
8	164/345	180/345	$\frac{4.7}{4.34}$	$\frac{0.499997}{0.49998}$	$\frac{3 \cdot 10^{-6}}{2 \cdot 10^{-5}}$

No. of elements	Frame on Fig. 6a, $\frac{\sigma_e / \varphi}{R_y}, \text{ MPa}$	Frame on Fig. 6b, $\frac{\sigma_e / \varphi}{R_y}, \text{ MPa}$	$\frac{\beta_1 \text{ (fig. 6, a)}}{\beta_2 \text{ (fig. 6, b)}}$	$\frac{\Phi(\beta_1)}{\Phi(\beta_2)}$	$\frac{P_{1dam,i}}{P_{2dam,i}}$
	Beams				
1	>1 <sup>1</sup>	294/375	$\frac{0}{2.13}$	$\frac{0}{0.4834}$	$\frac{0.5}{0.0166}$
2	>1	337/375	$\frac{0}{1.0}$	$\frac{0}{0.3413}$	$\frac{0.5}{0.1587}$
3	281/375	260/375	$\frac{2.47}{3.02}$	$\frac{0.4932}{0.4987}$	$\frac{0.0068}{0.0013}$
4	>1	313/375	$\frac{0}{1.63}$	$\frac{0}{0.4484}$	$\frac{0.5}{0.0516}$
5	269/375	300/375	$\frac{2.78}{1.97}$	$\frac{0.4973}{0.4756}$	$\frac{0.0027}{0.0244}$

<sup>1</sup>A beam is regarded as geometrically unstable when three or more plastic hinges form within its span as a result of deformation.

**Table 7. Calculation of the probability robustness index.**

No. of element s	Normal operation		Emergency situation, Fig. 6a / Fig. 6b		$P_{no,j} \left(1 - P_{dam,j}\right)$		$P_{no,i} \left(1 - P_{dam,i}\right)$		$\frac{W_{R1}}{W_{R2}}$
	Columns $P_{no,j}$	Beams $P_{no,i}$	Columns $\left(1 - P_{dam,j}\right)$	Beams $\left(1 - P_{dam,i}\right)$	Fig. 6a / Fig. 6b		Fig. 6a / Fig. 6b		
1	1	–	1/1	–	1	1	–	–	
2	1	–	-	–	–	–	–	–	
3	1	–	0.999997/1	–	0.999997	1	–	–	
4	1	–	0.9686/ 0.999997	–	0.9686	0.999997	–	–	
5	1	–	1/1	–	1	1	–	–	
6	1	–	0.834/1	–	0.834	1	–	–	
7	1	–	0.999997/ 0.9834	–	0.999997	0.9834	–	–	0.1
8	1	–	0.999997/ 0.9998	–	0.999997	0.9998	–	–	0.7516
1	–	0.999997	–	0.5/ 0.9834	–	–	0.49999	0.98339	
2	–	1	–	0.5/ 0.8413	–	–	0.5	0.8413	
3	–	0.999997	–	0.9932/ 0.9987	–	–	0.99319	0.99869	
4	–	0.999948	–	0.5/ 0.9484	–	–	0.49999	0.94839	
5	–	0.999968	–	0.9973/ 0.9756	–	–	0.99726	0.97558	

The calculation results demonstrated the critical importance of diagonal bracing 10 (see Figs. 2 and 6b) in ensuring structural robustness under the given accidental scenario. Verification analyses were performed using a nonlinear formulation, which showed that, in the absence of the diagonal element, the

system transformed into a mechanism and collapsed at 0.9 of the service load level. This confirms the earlier prediction that the robustness condition, whether according to equality  $W_R \approx 0.1 < 0.55$  or criterion

$$\left( \left( \prod_{i=1}^{m_R} (w_i) \right) = 0.1238 \right) \wedge \left( \prod_{j=1}^{m_c} (w_j) = 0.807 \right) \leq 0.6,$$

is not satisfied. Here, the value 0.1238 was obtained as the product of the reliability values for the beams (Column 8 in Table 7), and 0.807 as the product for the columns (Column 6 in Table 7). In the case of the system with the diagonal element included, it was established that the frame was capable of carrying the load under the accidental scenario without full collapse. Plastic hinges formed at the beam-to-left-column joints on all floors, while the maximum system deflection was 14.89 cm. Thus, the prediction based on the probabilistic robustness indicator was confirmed:  $W_R \approx 0.7516 > 0.55$ . The robustness condition was satisfied, as was the condition for groups of structural elements:

$$\left( \left( \prod_{i=1}^{m_R} (w_i) \right) = 0.7644 \right) \wedge \left( \prod_{j=1}^{m_c} (w_j) = 0.9832 \right) > 0.6.$$

### 3.3.3. Accidental Scenario C

Following the same procedure, it was established that under this accidental scenario, the system remains geometrically stable both with and without the diagonal element. As a first step, we assess the robustness of the frame without the diagonal element, accompanied by a corresponding verification analysis. If robustness is confirmed in this case, further evaluation of the system with the diagonal element becomes unnecessary. The results of the preliminary quasi-static analysis are shown in Fig. 7a. The calculation of the failure probability elements is given in Table 8.

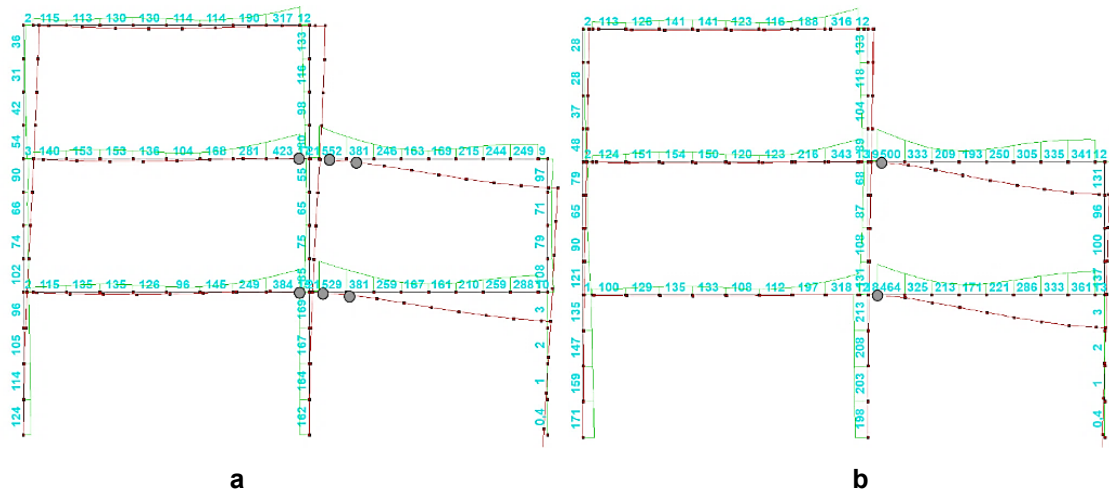


**Figure 7. Diagrams of equivalent quasi-static stresses (MPa) and deformed frame diagrams: a) linear calculation; b) physically and geometrically non-linear calculation.**

**Table 8. Calculation of the value  $P_{dam}$  (Scenario C).**

No. of elements	$\frac{\sigma_e/\varphi}{R_y}$ , MPa	$\beta_R$	$\Phi(\beta_b)$	$P_{dam,i}$
Columns				
1	124/337.5	$\beta > 5$	0.5	0
2	169/337.5	4.43	0.499997	$3.0 \cdot 10^{-6}$
3	—	—	—	—
4	102/345	$\beta > 5$	0.5	0
5	85/345	same	same	same
6	108/345	—/—	—/—	—/—
7	54/345	—/—	—/—	—/—
8	133/345	—/—	—/—	—/—



No. of elements	$\frac{\sigma_e/\varphi}{R_y}$ , MPa	$\beta_R$	$\Phi(\beta_b)$	$P_{dam,i}$
Beams				
1	249/375	3.31	0.49945	0.00055
2	288/375	2.28	0.4887	0.0113
3	281/375	2.47	0.4933	0.0067
4	246/375	3.39	0.4996	0.0004
5	317/375	1.52	0.4357	0.0643

Using the data from Tables 4 and 8, obtained:

$$W_R = \prod_{i=1}^5 \left( P_{no,i} (1 - P_{dam,i}) \right) \prod_{j=1}^8 \left( P_{no,j} (1 - P_{dam,j}) \right);$$

$$W_R \approx 0.999997 \cdot (1 - 0.00055) \cdot 1 \cdot (1 - 0.0113) \cdot 0.999997 \cdot (1 - 0.0067) \cdot 0.999948 \cdot (1 - 0.0004) \times \\ \times 0.999968 \cdot (1 - 0.0643) \cdot 1 \cdot (1 - 3 \cdot 10^{-6}) \approx 0.9179.$$

The robustness condition is satisfied,  $W_R \approx 0.9179 > 0.55$ . The nonlinear finite element analysis confirmed that under this accidental scenario, the system exhibits robustness. Two plastic hinges form in the beams, and the maximum deflection reaches 48.8 cm. Given a story height of 280 cm, such deflection may still allow for safe evacuation of occupants and removal of equipment. It should be noted that in this particular case, robustness is ensured by a design solution that involves a small degree of cantilever action in the building frame, which can be sustained by the beams. In other cases – for example, under increased loading – the installation of a diagonal bracing becomes necessary to enable redistribution of internal forces.

### 3.3.4. Accidental Scenario D

Initially, condition (3) is checked. Depending on the kinetic energy transferred to the beam and its actual SSS, the beam may resist the accidental load by forming a system of plastic hinges at the limit state, thereby creating a kinematic chain and acting as part of the frame similarly to a cable element. This mechanism is realized if condition (3) is not satisfied. If the condition is satisfied, a crack forms in the beam, which propagates and leads to fracture of the structural element. For definiteness, it is assumed that the beam contains a microdefect in the support joint, where the fracture initiates (see Fig. 8).

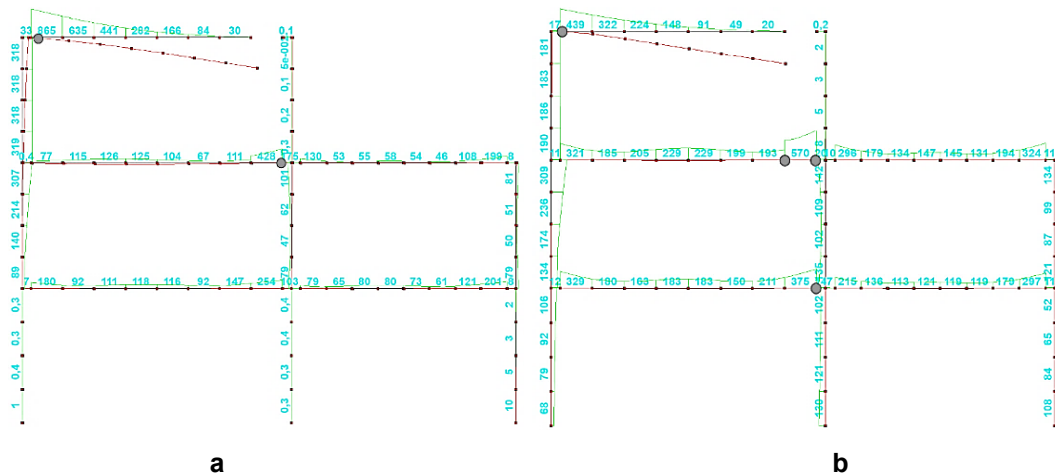


**Figure 8. Distributions of equivalent quasi-static stresses (MPa) and deformed configurations of the frame: a) linear analysis; b) physically and geometrically nonlinear analysis.**

An approximate evaluation of the integral in this particular case, considering the I-beam cross-section and the lateral bending condition, can be performed using the following expression derived from transformations of formula (3):

$$J = 2 \sum_{n_{\Delta}} \int_0^{\Delta_i} \left( \frac{\Delta P_i}{2hb_i} + \frac{\Delta \sigma_{s0i} R_u h}{b_i R_s} \right) d\Delta_i, \quad (16)$$

$$\sigma_{s0} = \sqrt{\left(\frac{\sigma_z + \sigma_y}{2}\right)^2 + 3\left(\frac{\sigma_z - \sigma_y}{2}\right)^2 + 3\tau_{zy}^2}, \quad (17)$$

where:  $i$  is the displacement  $\Delta_i$  increment number;  $i=1 \dots n_\Delta$ ,  $n_\Delta$  is the number of displacement increments into which the total displacement  $\Delta$  of the rod with a growing crack is divided;  $\Delta P_i$ ,  $\Delta \sigma_{s0i}$  are the load increment causing the displacement  $\Delta_i$  increment, and the equivalent stress increment;  $b_i$  is the distance from the crack tip to the opposite edge of the cross-section;  $h$  is the actual width of the sheet in which the crack growth condition is checked;  $R_s$ ,  $R_u$  are the calculated resistances of steel, determining its yield and rupture;  $\Delta \sigma_{s0i}$  is the increment of Mises stresses;  $\sigma_z$ ,  $\sigma_y$ ,  $\tau_{zy}$  are the components of normal and shear stresses.

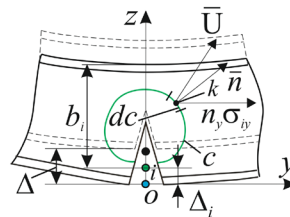


**Figure 9. Crack growth pattern in an I-beam section.**

Calculations showed that, under the values of the vertical dynamic load (see Fig. 2) acting on the roof beam –specifically, when the load magnitude is  $P_D \geq 120$  kN, converted to a static equivalent using a factor of 2 – a progressive, unstable crack growth occurs, eventually leading to fracture of the beam section. As a result, part of the load is transferred to the lower beam. Under this assumed failure mechanism, the analytical model can be modified using contact elements to accurately represent the load transfer. However, since such modeling features are beyond the scope of this paper, they are not considered here. Approximately 5/6 of the static equivalent of the accidental load – i.e., about 100 kN – is transmitted to the lower beam through the contact point. The analytical model for evaluating the probabilistic robustness indicator is shown in Fig. 8, and the reliability index calculations are presented in Table 9. As is evident even from the linear quasi-static analysis (see Fig. 8a), fracture of the upper beam causes significant additional bending moment loading in the left-hand column of the two adjacent stories. The results of the nonlinear analysis further confirm that moment redistribution occurs toward the first-story beam, where a plastic hinge forms at the support section (see Fig. 8b).

**Table 9. The calculation of the value  $P_{dam}$  (Scenario D).**

No. of elements	$\frac{\sigma_e/\varphi}{R_y}$ , MPa	$\beta_R$	$\Phi(\beta_b)$	$P_{dam,i}$
Columns				
1	1/337.5	$\beta > 5$	0.5	0
2	0.4/337.5	same	same	same
3	10/337.5	-/-	-/-	-/-
4	307/345	1.00	0.3413	0.1587
5	101/345	$\beta > 5$	0.5	0
6	81/345	same	same	same
7	319/345	0.68	0.2517	0.2483
8	0.3/345	$\beta > 5$	0.5	0
Beams				
1	254/375	3.18	0.4992	0.0008
2	201/375	4.57	0.499997	$3.0 \cdot 10^{-6}$
3	199/375	4.63	0.499997	$3.0 \cdot 10^{-6}$
4	126/375	$\beta > 5$	0.5	0
5	–	–	–	–

Accounting the possible sequential failure of Beam 3 and Beam 1, we obtain the following result:

$$W_R = \prod_{i=1}^8 \left( P_{no,i} (1 - P_{dam,i}) \right) \left[ P_{no,1} (1 - P_{dam,1} P_{dam,3}) \right] \prod_{j=2}^5 \left( P_{no,j} (1 - P_{dam,j}) \right) = 0.6318 > 0.55.$$

Under this accidental scenario, the system demonstrates structural robustness. This prediction is fully confirmed by the nonlinear analysis.

#### 4. Discussion and Research Prospects

The robustness condition of the system  $W_R > 0.55$  may be revised depending on the type of the structural system considered and the criteria used for assessing the structure's performance. However, calculations have shown that for steel frame structural systems subjected to loads typically experienced by buildings and constructions, this condition holds true. The issue of the initial quasi-static assessment of the structure, upon which the robustness forecast is based, remains debatable. Nevertheless, joint evaluations of the system's geometric variability with plastic hinges and numerous calculations of such systems have never revealed discrepancies between the forecast and subsequent analyses accounting for physical, geometric, and structural nonlinearities.

There are known studies, in which robustness is evaluated based on the satisfaction of boundary inequalities [10], as well as using deterministic [56] and probabilistic indicators [57]. The survivability assessments of frame structures obtained using these methodologies are in good agreement with the qualitative evaluation of robustness presented in this paper.

The prospects of the current work lie in extending the theoretical framework to other types of building frames, including high-rise and unique structures. It is advisable to consider not only the design stage aimed at preventing possible accidents but also the normal operational period of the structural system, during which damage may accumulate due to both mechanical impacts (overloads, reconfigurations, etc.) and environmental effects, such as corrosion damage. Besides column removal, emergency scenarios can include standard fire exposure and various corrosion damage scenarios.

#### 5. Conclusions

1. A new methodology for the quantitative assessment of the robustness of steel frame systems has been developed, based on a probabilistic index that accounts for the possibility of reliable operation of some structural elements and the failure of individual elements within the localization zone of accidental impact.
2. The applicability of the proposed methodology is demonstrated using various scenarios of accidental impact localization on a steel frame with I-section profiles, enabling the evaluation of robustness for both newly designed and rehabilitated steel structural systems.
3. The proposed methodology illustrates the potential for applying different strategies to strengthen the structural system or enhance its resistance to progressive collapse. In particular, the highly effective role of diagonal bracing elements in frames is confirmed, which is consistent with other research findings. Additionally, it is shown that increasing the cross-sectional size of elements is not advisable in a catenary progressive collapse localization scheme.

#### References

1. Emamikoupaei, A., Tsavdaridis, K.D., Bigdeli, A., Saffarzadeh, K. Fragility-Based Robustness Assessment of Steel Modular Building Systems: Connection and Building Height. *Journal of Constructional Steel Research*. 2025. 226. Article no. 109199. DOI: 10.1016/J.JCSR.2024.109199
2. Rodríguez, D., Brunesi, E., Nascimbene, R. Fragility and Sensitivity Analysis of Steel Frames with Bolted-Angle Connections under Progressive Collapse. *Engineering Structures*. 2021. 228. Article no. 111508. DOI: 10.1016/j.engstruct.2020.111508
3. Li, L.L., Li, G.Q., Jiang, B., Lu, Y. Analysis of Robustness of Steel Frames against Progressive Collapse. *Journal of Constructional Steel Research*. 2018. 143. Pp. 264–278. DOI: 10.1016/J.JCSR.2018.01.010
4. Xie, Z., Chen, Y. Numerical Study of the Robustness of Steel Moment Connections under Catenary Effect. *Engineering Structures*. 2022. 252. Article no. 113658. DOI: 10.1016/j.engstruct.2021.113658
5. Wang, Y., Li, J., Bai, C., Shen, H., Tian, L. Novel Beam–Column Joint with the Folded Plates for Improving Progressive Collapse Resistance of Steel-Frame Structures. *Structures*. 2024. 61. Article no. 106047. DOI: 10.1016/J.ISTRUC.2024.106047
6. Kozłowski, A., Kukla, D. Numerical Investigation of Steel Frame Robustness under External Sudden Column Removal. *Archives of Civil Engineering*. 2023. 69 (2). Pp. 177–193. DOI: 10.24425/ace.2023.145262

7. Wang, X., Wang, P., Chen, W. Test on Progressive Collapse of Steel Moment-Resisting Frame with Upper-and-Lower Flange Angle Steel Connection. *Structures*. 2024. 68. Article no. 107171. DOI: 10.1016/J.ISTRUC.2024.107171
8. Kukla, D., Kozłowski, A. Numerical Study of the Robustness of Steel Frames with Bolted End-Plate Joints Subjected to Sudden and Gradual Internal Column Loss. *International Journal of Steel Structures*. 2023. 23. Pp. 1211–1222. DOI: 10.1007/s13296-023-00761-z
9. Possidente, L., Freddi, F., Tondini, N. Dynamic Increase Factors for Progressive Collapse Analysis of Steel Structures Considering Column Buckling. *Engineering Failure Analysis*. 2024. 160. Article no. 108209. DOI: 10.1016/J.ENGFAILANAL.2024.108209
10. Lan, X., Li, Z., Fu, F., Qian, K. Robustness of Steel Braced Frame to Resist Disproportionate Collapse Caused by Corner Column Removal. *Journal of Building Engineering*. 2023. 69. Article no. 106226. DOI: 10.1016/J.JOBE.2023.106226
11. Ma, Y.X., Chen, S., Tan, K.H. Experimental Study of Steel Beam-Column Joints with Novel Slot-Bolted Connections under a Central-Column-Removal Scenario. *Journal of Constructional Steel Research*. 2024. 214. Article no. 108481. DOI: 10.1016/j.jcsr.2024.108481
12. Guo, Y., Yang, B., Alqawzai, S., Chen, K., Kong, D. Machine Learning-Based and Interpretable Models for Predicting the Resistance and Probability of Progressive Collapse of Steel Frame-Composite Floor Structures. *Engineering Structures*. 2025. 332. Article no. 120089. DOI: 10.1016/J.ENGSTRUCT.2025.120089
13. Miao, X., Wang, Y., Peng, L., Zhao, Y. Feature Extraction and Quantitative Analysis of Steel Corrosion in Reinforced Concrete Components Based on XCT Scanning and Deep Learning Model. *Journal of Building Engineering*. 2025. 106. Article no. 112652. DOI: 10.1016/J.JOBE.2025.112652
14. Lin, K., Chen, Z., Li, Y., Lu, X. Uncertainty Analysis on Progressive Collapse of RC Frame Structures under Dynamic Column Removal Scenarios. *Journal of Building Engineering*. 2022. 46. Article no. 103811. DOI: 10.1016/j.jobe.2021.103811
15. Zhu, X., Ou, G. Wind Fragility Modeling of Transmission Tower-Line System Based on Threat-Dependent Structural Robustness Index. *Structural Safety*. 2025. 114. Article no. 102571. DOI: 10.1016/J.STRUSAFE.2024.102571
16. Khayatizad, M., Honhon, M., De Waele, W. Detection of Corrosion on Steel Structures Using an Artificial Neural Network. *Structure and Infrastructure Engineering*. 2023. 19 (12). Pp. 1860–1871. DOI: 10.1080/15732479.2022.2069272
17. Roshani, M. Quantification of Structural and Non-Structural Robustness of Tall Steel Buildings Using a Straightforward Methodology. *Structures*. 2024. 62. Article no. 106220. DOI: 10.1016/j.istruc.2024.106220
18. Noruzvand, M., Mohebbi, M., Shakeri, K. Performance-Based Seismic Design of Low-Rise Steel Moment-Resisting Frames Targeting Collapse Fragility Curve. *Structures*. 2024. 70. Article no. 107630. DOI: 10.1016/J.ISTRUC.2024.107630
19. Jiang, L., Ye, J. Risk-Based Overall Seismic Robustness Assessment of Cold-Formed Steel Structures Considering Vulnerability and Fragility. *Bulletin of Earthquake Engineering*. 2022. 20. Pp. 7161–7184. DOI: 10.1007/s10518-022-01435-7
20. Tavakoli, H.R., Afrapoli, M.M. Robustness Analysis of Steel Structures with Various Lateral Load Resisting Systems under the Seismic Progressive Collapse. *Engineering Failure Analysis*. 2018. 83. Pp. 88–101. DOI: 10.1016/j.engfailanal.2017.10.003
21. Formisano, A., Landolfo, R., Mazzolani, F.M. Robustness Assessment Approaches for Steel Framed Structures under Catastrophic Events. *Computers & Structures*. 2015. 147. Pp. 216–228. DOI: 10.1016/j.compstruc.2014.09.010
22. Solgi, M., Rajabi, E., Amiri, G.G., Raissi Dehkordi, M. Seismic Resilience Evaluation of a 3D Steel Moment Frame Building with Triple Friction Pendulum Isolators. *Structures*. 2025. 72. Article no. 108075. DOI: 10.1016/J.ISTRUC.2024.108075
23. Mozafari, N., Hashemi, S.S., Jahangiri, M., Vaghefi, M., Javidi, S. Assessment of Progressive Collapse Mechanisms in Cold-Formed Steel-Framed Structures Facing Multi-Element Initial Damage Conditions. *Structures*. 2025. 78. Article no. 109343. DOI: 10.1016/J.ISTRUC.2025.109343
24. Naji, A. Robustness of Steel Moment Frames against Progressive Collapse by Means of Plastic Limit Analysis. *International Journal of Structural Integrity*. 2020. 11 (2). Pp. 264–276. DOI: 10.1108/IJSI-06-2019-0051
25. Xie, D., Xu, Y., Nadarajan, S., Viswanathan, V., Gupta, A.K. Robust Stability-Constrained Optimization for Load Restoration with Uncertain Dynamic Loads. *Applied Energy*. 2025. 395. Article no. 126070. DOI: 10.1016/J.APENERGY.2025.126070
26. Barros, B., Conde, B., Cabaleiro, M., Riveiro, B. Design and Testing of a Decision Tree Algorithm for Early Failure Detection in Steel Truss Bridges. *Engineering Structures*. 2023. 289. Article no. 116243. DOI: 10.1016/j.engstruct.2023.116243
27. Suwondo, R., Cunningham, L., Gillie, M., Suangga, M., Hidayat, I. Improving the Robustness of Steel Frame Structures under Localised Fire Conditions. *Journal of Structural Fire Engineering*. 2022. 13 (3). Pp. 307–320. DOI: 10.1108/JSFE-07-2021-0046
28. Yang, Z., Yang, Q., Lu, W.Z. DeepMonte-Frame: An Intelligent Workflow for Planar Steel Frame Design Based on Monte Carlo Tree Search and Feedforward Neural Networks. *Advanced Engineering Informatics*. 2025. 66. Article no. 103510. DOI: 10.1016/J.AEI.2025.103510
29. Kirsanov, M.N. Formula for Calculation of the Deflection of a Flat Strut Bridge with an Arbitrary Number of Panels. *Structural Mechanics and Analysis of Constructions*. 2022. 302 (3). Pp. 9–13. DOI: 10.37538/0039-2383.2022.3.9.13
30. Kirsanov, M.N. Formulas for Calculating Deformations and Natural Frequency of Free Vibrations of a Hexagonal Tower. *Russian Journal of Building Construction and Architecture*. 2024. 1 (61). Pp. 101–109. DOI: 10.36622/vstu.2024.61.1.009
31. Kaveh, A., Biabani Hamedani, K., Milad Hosseini, S., Bakhshpoori, T. Optimal Design of Planar Steel Frame Structures Utilizing Meta-Heuristic Optimization Algorithms. *Structures*. 2020. 25. Pp. 335–346. DOI: 10.1016/j.istruc.2020.03.032
32. Alekseytsev, A.V., Akhremenko, S.A. Evolutionary Optimization of Prestressed Steel Frames. *Magazine of Civil Engineering*. 2018. 5 (81). Pp. 32–42. DOI: 10.18720/MCE.81.4
33. Tamrazyan, A., Alekseytsev, A. Evolutionary Optimization of Reinforced Concrete Beams, Taking into Account Design Reliability, Safety and Risks during the Emergency Loss of Supports. *E3S Web of Conferences*. 2019. 97. Article no. 04005. DOI: 10.1051/e3sconf/20199704005
34. Alekseytsev, A.V., Kurchenko, N.S. Deformations of Steel Roof Trusses under Shock Emergency Action. *Magazine of Civil Engineering*. 2017. 5 (73). Pp. 3–13. DOI: 10.18720/MCE.73.1
35. Shan, W., Liu, J., Zhou, J. Integrated Method for Intelligent Structural Design of Steel Frames Based on Optimization and Machine Learning Algorithm. *Engineering Structures*. 2023. 284. Article no. 115980. DOI: 10.1016/j.engstruct.2023.115980
36. RahmaniKhah, A., Mahmoudi, M., Zayeri Baghlani Nejad, A. Structural Damage Identification Using Model Updating, Hybrid Optimization Algorithms, and Incomplete Mode Shapes. *Structures*. 2025. 77. Article no. 109209. DOI: 10.1016/J.ISTRUC.2025.109209

37. El Hajj Diab, M., Desprez, C., Orcesi, A., Bleyer, J. Structural Robustness Quantification through the Characterization of Disproportionate Collapse Compared to the Initial Local Failure. *Engineering Structures*. 2022. 255. Article no. 113869. DOI: 10.1016/j.engstruct.2022.113869
38. Kaveh, A., Zaeerza, A. Optimum Design of the Frame Structures Using the Force Method and Three Recently Improved Metaheuristic Algorithms. *International Journal of Optimization in Civil Engineering*. 2023. 13 (3). Pp. 309–325. DOI: 10.22068/ijoc.2023.13.3.556
39. Kanyilmaz, A., Berto, F. Robustness-Oriented Topology Optimization for Steel Tubular Joints Mimicking Bamboo Structures. *Material Design and Processing Communications*. 2019. 1. Article no. e43. DOI: 10.1002/mdp2.43
40. Kalapodis, N.A., Muho, E.V., Beskos, D.E. Structure-Specific, Multi-Modal and Multi-Level Scalar Intensity Measures for Steel Plane Frames. *Soil Dynamics and Earthquake Engineering* 2025. 190. Article no. 109185. DOI: 10.1016/J.SOILDYN.2024.109185
41. Jiang, B., Wang, M., Shen, Y., Li, Y. Robustness Assessment of Planar Steel Frames Caused by Failure of a Side Column under Localized Fire. *The Structural Design of Tall and Special Buildings*. 2020. 29. Article no. e1711. DOI: 10.1002/tal.1711
42. Jiang, B., Li, G.Q., Yam, M.C.H. Simplified Robustness Assessment of Steel Framed Structures under Fire-Induced Column Failure. *Steel and Composite Structures*. 2020. 35 (2). Pp. 199–213. DOI: 10.12989/scs.2020.35.2.199
43. Freddi, F., Ciman, L., Tondini, N. Retrofit of Existing Steel Structures against Progressive Collapse through Roof-Truss. *Journal of Constructional Steel Research*. 2022. 188. Article no. 107037. DOI: 10.1016/j.jcsr.2021.107037
44. Li, Z., Xue, T., Li, G., Lan, X., Qian, K. Influence of Steel Braces on Robustness of Multilayer Steel Frames against Progressive Collapse. *Jianzhu Jieqou Xuebao/Journal of Building Structures*. 2023. 44 (4). Pp. 257–266. DOI: 10.14006/j.jzjgxb.2021.0824
45. Shokoohimatin, M., Hosseini, M., Firoozi Nezamabadi, M. The Effect of Plan Geometry on Progressive Collapse of Tall Buildings with Diagrid Structure Based on Nonlinear Static and Dynamic Analyses. *International Journal of Steel Structures*. 2024. 24. Pp. 217–230. DOI: 10.1007/s13296-023-00801-8
46. Yang, X., Ma, R., Bi, K., Li, H., Du, X. Effectiveness and Robustness of Using Nonlinear Pendulum Tuned Mass Damper Inerters for Wind-Induced Vibration Mitigation of High-Rise Buildings. *Structures*. 2025. 73. Article no. 108356. DOI: 10.1016/J.ISTRUC.2025.108356
47. Jakab, D., Marginean, I., Dubina, D. Robustness capacity of multistorey steel structures in case of fire after earthquake events. *Proceedings of the Romanian Academy Series A – Mathematics Physics Technical Sciences Information Science*. 2023. 24 (1). Pp. 71–78. DOI: 10.59277/prs-ser.a.24.1.09
48. Zhang, J.Z., Deng, Y.T., Li, G.Q., Yu, Z.W. Robustness of Column-Supported Modular Steel Buildings in Column Loss: Role of Double-Layer Beams and Point-Restrained Slabs. *Engineering Structures*. 2025. 329. Article no. 119786. DOI: 10.1016/J.ENGSTRUCT.2025.119786
49. Li, H., Zhong, C., Hui, Z. Reliability Assessment of Stainless Steel Columns under Axial Compression. *Structures*. 2025. 72. Article no. 108257. DOI: 10.1016/J.ISTRUC.2025.108257
50. Alembagheri, M., Sharafi, P., Tao, Z., Hajirezaei, R., Kildashti, K. Robustness of Multistorey Corner-Supported Modular Steel Frames against Progressive Collapse. *Structural Design of Tall and Special Buildings*. 2021. 30. Article no. e1896. DOI: 10.1002/tal.1896
51. Zhang, J.Z., Jiang, B.H., Feng, R., Chen, R. Robustness of Steel Moment Frames in Multi-Column-Removal Scenarios. *Journal of Constructional Steel Research*. 2020. 175. Article no. 106325. DOI: 10.1016/J.JCSR.2020.106325
52. Shan, S., Pan, W. Progressive Collapse Mechanisms of Multi-Storey Steel-Framed Modular Structures under Module Removal Scenarios. *Structures*. 2022. 46. Pp. 1119–1133. DOI: 10.1016/j.istruc.2022.10.106
53. Zhang, J.Z., Deng, Y.T., Li, G.Q., Yu, Z.W. Robustness of Column-Supported Modular Steel Buildings in Column Loss: Role of Double-Layer Beams and Point-Restrained Slabs. *Engineering Structures*. 2025. 329. Article no. 119786. DOI: 10.1016/J.ENGSTRUCT.2025.119786
54. Zhang, J.Z., Chen, X., Zhang, W.J., Li, G.Q., Yu, Z.W. Collapse Resistance of Floor System in Steel Modular Structure. *Thin-Walled Structures*. 2024. 197. Article no. 111664. DOI: 10.1016/j.tws.2024.111664
55. Wang, J., Ke, K., Wang, W. Structural Robustness Evaluation of Steel Frame Buildings with Different Composite Slabs Using Reduced-Order Modeling Strategies. *Journal of Constructional Steel Research*. 2022. 196. Article no. 107371. DOI: 10.1016/J.JCSR.2022.107371
56. Rice, J.R. A Path Independent Integral and the Approximate Analysis of Strain Concentration by Notches and Cracks. *ASME. Journal of Applied Mechanics*. 1968. 35 (2). Pp. 379–386. DOI: 10.1115/1.3601206
57. Emamikoupaei, A., Tsavdaridis, K.D., Bigdeli, A., Saffarzadeh, K. Fragility-based robustness assessment of steel modular building systems: Connection and building height. *Journal of Constructional Steel Research*. 2025. 226. Article no. 109199. DOI: 10.1016/J.JCSR.2024.109199

#### **Information about authors:**

**Anatoly Alekseytsev, Doctor of Technical Sciences**

ORCID: <https://orcid.org/0000-0002-4765-5819>

E-mail: [aalexw@mail.ru](mailto:aalexw@mail.ru)

**Natalya Kurchenko, PhD in Technical Sciences**

ORCID: <https://orcid.org/0000-0002-5434-4277>

E-mail: [ms.kurchenko@mail.ru](mailto:ms.kurchenko@mail.ru)

*Received 06.06.2025. Approved after reviewing 02.08.2025. Accepted 05.08.2025.*